Primary Steps in the Energy Conversion Reaction of the Cytochrome bc_1 Complex Q_O Site[1]

R. Eryl Sharp,[2] Christopher C. Moser,[2] Brian R. Gibney,[2] and P. Leslie Dutton[2,3]

The primary energy conversion (Q_O) site of the cytochrome bc_1 complex is flanked by both high- and low-potential redox cofactors, the [2Fe–2S] cluster and cytochrome b_L, respectively. From the sensitivity of the reduced [2Fe–2S] cluster electron paramagnetic resonance (EPR) spectral g_x-band and line shape to the degree and type of Q_O site occupants, we have proposed a double-occupancy model for the Q_O site by ubiquinone in *Rhodobacter capsulatus* membrane vesicles containing the cytochrome bc_1 complex. Biophysical and biochemical experiments have confirmed the double occupancy model and from a combination of these results and the available cytochrome bc_1 crystal structures we suggest that the two ubiquinone molecules in the Q_O site serve distinct catalytic roles. We propose that the strongly bound ubiquinone, termed Q_{OS}, is close to the [2Fe–2S] cluster, where it remains tightly associated with the Q_O site during turnover, serving as a catalytic cofactor; and the weaker bound ubiquinone, Q_{OW}, is distal to the [2Fe–2S] cluster and can exchange with the membrane Q_{pool} on a time scale much faster than the turnover, acting as the substrate. The crystallographic data demonstrates that the FeS subunit can adopt different positions. Our own observations show that the equilibrium position of the reduced FeS subunit is proximal to the Q_O site. On the basis of this, we also report preliminary results modeling the electron transfer reactions that can occur in the cytochrome bc_1 complex and show that because of the strong distance dependence of electron transfer, significant movement of the FeS subunit must occur in order for the complex to be able to turn over at the experimental observed rates.

KEY WORDS: Q_O site; ubiquinone binding; electron paramagnetic resonance; inhibitors; electron transfer.

INTRODUCTION

The primary energy conversion reaction of the cytochrome bc_1 complex occurs at the Q_O site and involves the two-electron oxidation of ubihydroqui-none (QH_2) to ubiquinone (Q) (Brandt and Trumpower, 1994; Gray and Daldal, 1995). The key facet of this reaction is the obligatory bifurcation of electron transfer along both a high- and low-potential redox chain by the cooperation of two one-electron redox centers that flank the Q_O site, the [2Fe–2S] cluster and cyt b_L, respectively (Fig. 1). As dictated in the Q-cycle model originally proposed by Mitchell (Mitchell, 1975), two QH_2 molecules must be oxidized at the Q_O site in order for complete turnover of the cyt bc_1 complex to occur (Lawford and Garland, 1983; Crofts and Wraight, 1983). The conventional model for Q_O site catalysis envisions the Q_O site as binding one QH_2 at a time and performing two separate, serial catalytic oxidations including the attendant binding and release steps. However, despite intensive investigation of Q_O
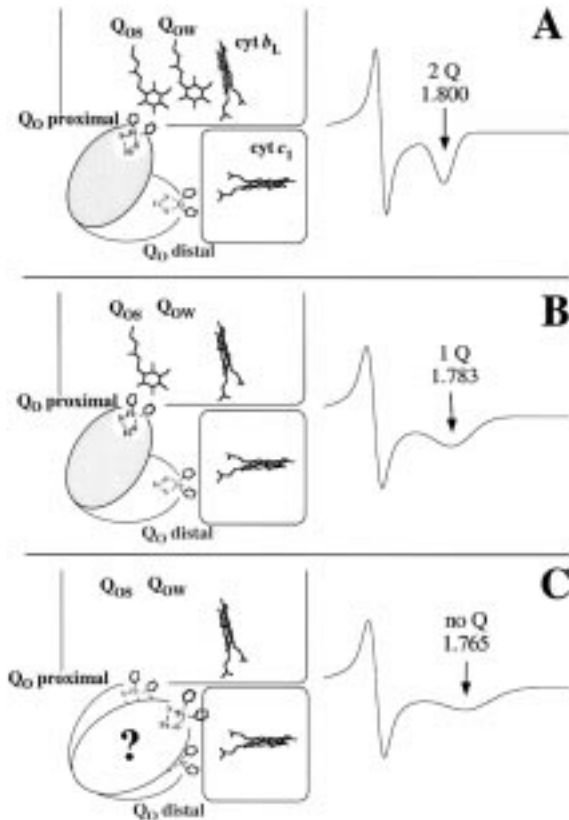
Fig. 1. Structural interpretation of the Q_O site occupancy and correlation with the reduced [2Fe–2S] cluster EPR spectra. Panels A to C represent different Q_O site ubiquinone occupancies. The left-hand side shows a schematic representation for the region of the cyt bc_1 complex surrounding the Q_O site, based on the crystal structure data. On the right-hand side, the characteristic [2Fe–2S] cluster EPR spectral line shape is depicted, which has previously been shown to be dependent upon the number of ubiquinone occupants in the Q_O site (Ding *et al.*, 1992). (A) Two ubiquinones in the Q_O site: the FeS subunit is positioned so that the [2Fe–2S] cluster is close to the Q_{OS} ubiquinone (Q_O proximal), the narrow EPR line shape has a g_x resonance centered at 1.800. (B) One ubiquinone in the Q_O site: the FeS subunit position is still Q_O proximal, but the EPR line shape is now indicative of one ubiquinone in the Q_{OS} site only, with a g_x band at 1.783. (C) Q_O site devoid of ubiquinone: the FeS subunit equilibrium position is no longer necessarily biased toward the Q_O site; the [2Fe–2S] cluster may be interacting with water and in an uncertain position. We show the FeS subunit as being positionally averaged between the Q_O proximal and distal positions, the broad g_x resonance is centered at 1.765.

site function, the fundamental mechanistic features of this centrally important reaction (substrate stoichiometry and reaction dynamics) still remain to be unambiguously resolved (Crofts and Wang, 1989; Brandt *et al.*, 1991; Brandt and von Jagow, 1991; Ding *et al.*, 1992,

1995; Brandt, 1996; a, b, 1998; Brandt and Djafarzadeh-Andabili, 1997; Brandt and Okun, 1997; Crofts and Berry, 1998; Junemann *et al.*, 1998; Crofts *et al.*, 1999; Sharp *et al.*, 1999a). The determination of high resolution structures for the cyt bc_1 complex by various groups has confirmed the general Q_O site locality defined from biochemical studies of native cyt bc_1 structures, but has not yet been able to resolve the question of the actual Q_O site ubiquinone stoichiometry (Xia *et al.*, 1997; Iwata *et al.*, 1998; Kim *et al.*, 1998; Zhang *et al.*, 1998). In this review we highlight recent biochemical experiments performed in our laboratory on native cyt bc_1 complexes in *Rhodobacter capsulatus* chromatophore membranes to probe Q_O site function. Specifically, we address Q_O site substrate stoichiometry, functionality, electron transfer parameters and relate our data with the emerging structural information to provide a consistent model for Q_O site activity.

Q_O SITE SUBSTRATE STOICHIOMETRY

Progress into investigating the Q_O site substrate binding capacity has been provided by the electron paramagnetic resonance (EPR) spectral line shape, and especially the g_x band of the reduced [2Fe–2S] cluster of the cyt bc_1 complex. These spectral parameters are extremely sensitive to the stoichiometry and nature of the Q_O site occupants, whether it be Q, QH_2, inhibitors, or other small molecules (Ding *et al.*, 1992). In order to investigate the binding of ubiquinone to the Q_O site, the distinctive EPR line shapes of the [2Fe–2S] cluster were modulated by manipulating the amount of ubiquinone present in the Q_O site. This was accomplished in three ways: (1) using chromatophore membranes with varying amounts of ubiquinone in the pool from the prevailing native concentration of about 30 mM down to zero — achieved by solvent extraction and reconstitution of ubiquinone (Ding *et al.*, 1992); (2) using cyt bc_1 complexes with Q_O site mutations that disrupt ubiquinone binding (Ding *et al.*, 1995); and (3) utilizing a combination of inhibitor binding and Q-extraction studies (Sharp *et al.*, 1999a, b).

Probing Q_O Site Occupancy by Q Extraction from Membranes

In approach (1), the EPR data obtained from the Q-extraction studies was deconvoluted and best interpreted in terms of two ubiquinone species, which

bound to the Q$_O$ site with strong and weak affinity, termed Q$_{OS}$ and Q$_{OW}$, respectively (Fig. 1) (Ding *et al.*, 1992). The generic [2Fe–2S] cluster EPR spectra that have been ascribed to the two ubiquinone binding domains in the Q$_O$ site are illustrated in Fig. 1. In native chromatophores with the Q$_{pool}$ oxidized, the [2Fe–2S] cluster EPR line shape exhibits a prominent g_x resonance centered at 1.800; partial Q extraction results in the broadening and an upfield shift of the g_x resonance to 1.783; finally, upon complete Q extraction, further broadening and an upfield shift of the g_x resonance to 1.765 occurs (Ding *et al.*, 1992). It has been suggested that the intermediate state is a mixture of the two extreme states (Crofts *et al.*, 1999), but as illustrated in Fig. 2, this is clearly not the case. The data depicted in Fig. 2 also shows linear combinations of the g_x resonances at 1.800 (native Q$_{pool}$ levels) and 1.765 (fully Q extracted) to illustrate that the spectral line shape at a g_x value of 1.783 is *not* the average of the 1.800 and 1.765 signals, but instead represents a distinct state. Thus, these three unique [2Fe–2S] cluster EPR spectral line shapes must reflect a genuine
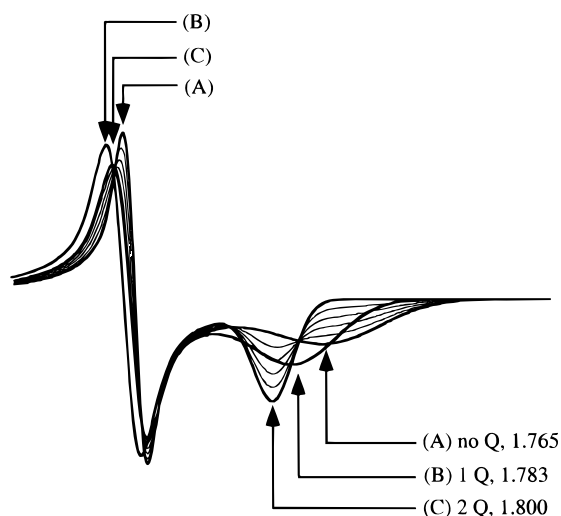

Fig. 2. The characteristic [2Fe–2S] cluster EPR spectra, illustrating the position of the g_x band and the line shape, which have previously been shown to be dependent upon the number of ubiquinone occupants in the Q$_O$ site: when two ubiquinones are resident in the Q$_O$ site, g_x = 1.800; with only one ubiquinone in the Q$_O$ site, g_x = 1.783; when the Q$_O$ site is completely devoid of ubiquinone, g_x = 1.765. Also illustrated is the fact that the EPR spectral lineshape centered at 1.783 is not a linear contribution of the 1.800 and 1.765 signals. The lighter spectral traces in between the 1.800 and 1.765 limits are generated by combing these signals in the proportions 1:0 (1.800:1.765), 4:1, 3:2, 2:3, 1:4, 0:1, respectively. The spectra were generated from simulating the experimental data using the program EPRSim XOP for Igor Pro (J. Boswell, Oregon Graduate Institute).

three-state transition, consistent with a binding site that accommodates two ubiquinone ligands with different binding affinities K_d(Q$_{OS}$) ~ 0.05 mM and K_d(Q$_{OW}$) ~ 1 mM. The simplest explanation for these phenomena remains that of hydrogen bonding interactions between the [2Fe–2S] cluster histidine ligands and the Q$_O$ site ubiquinone(s) (Ding *et al.*, 1992; Sharp *et al.*, 1998).

Probing Q$_O$ Site Occupancy by Site-Directed Mutation

The second approach studying the effect of a large number of Q$_O$ site mutations (F144X, G158X, where X corresponds to ten different amino acids substitutions) on the binding affinity of ubiquinone complements the Q-extraction approach and is again best interpreted in terms of a double occupancy model for the Q$_O$ site, generating a data set with a range of Q$_{OS}$ and Q$_{OW}$ domain occupancies in different mutants (Ding *et al.*, 1995). Furthermore, coupling of kinetic studies to the EPR analysis for ubiquinone occupancy in cyt *bc*$_1$ complexes with Q$_O$ site mutations has facilitated putative functional assignments for the Q$_{OS}$ and Q$_{OW}$ domains in Q$_O$ site catalysis. The yield of QH$_2$ oxidation correlates linearly with Q$_{OS}$ domain occupancy, implying that exchange of Q/QH$_2$ with the Q$_{pool}$ in the membrane is much slower than the time scale for catalytic turnover. However, the rate constants for oxidation of the first QH$_2$ in the catalytic cycle correlate with the K_d values for Q/QH$_2$ in the Q$_{OW}$ domain in a simple kinetic model in which exchange of Q/QH$_2$ with the Q$_{pool}$ is much faster than the time scale for turnover (~ 1700 s^{-1}). This implies that the Q$_{OS}$ domain can be envisioned as binding a cofactor ubiquinone, since this does not exchange with the Q$_{pool}$ on the catalytic time scale, and the Q$_{OW}$ domain as binding a substrate ubiquinone because this can exchange at a rate faster than the turnover.

Probing Q$_O$ Site Occupancy Using Site-Specific Inhibitors

This is the most recent approach that we have used, but combined with the Q-extraction studies, it is a powerful tool for analyzing Q$_O$ site substrate stoichiometry. (Sharp *et al.*, 1999a,b). The data presented in Fig. 3 show that addition of excess diphenylamine (DPA) or stoichiometric amounts of methoxyacrylate (MOA)-stilbene (relative to the cyt *bc*$_1$ complex concentration) to chromatophore membranes with native
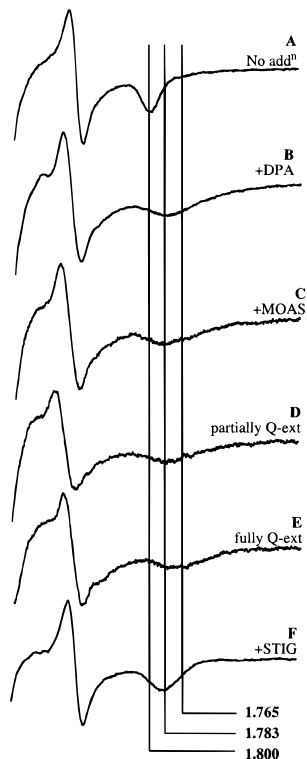
Fig. 3. Effect of Q_O site inhibitors and Q extraction on the reduced [2Fe–2S] cluster EPR spectrum in *R. capsulatus* chromatophores suspended in buffer solution (50 mM MOPS, 100 mM KCl, pH 7.0). Experimental conditions are described as previously described (Sharp *et al.*, 1999a). All samples were suspended to 20 μM cyt bc_1 concentration and the redox poise adjusted to 200 mV. At this potential the [2Fe–2S] cluster is $>$ 95% reduced and the Q_{pool} is fully oxidized. (A) Unextracted chromatophores with native level of ubiquinone ($\sim$ 30 per cyt bc_1 complex); (B) unextracted $+$ 100 mM DPA; (C) unextracted $+$ 20 μM MOA-stilbene; (D) partially Q-extracted chromatophores, $g_x = 1.783$; (E) fully Q-extracted chromatophores, $g_x = 1.765$; (F) unextracted $+$ 20 μM stigmatellin.

concentrations of ubiquinone results in the generation of a [2Fe–2S] cluster EPR spectral line shape that is identical to that for partially Q-extracted chromatophores, with a g_x resonance at 1.783. Moreover, addition of either excess DPA or stoichiometric MOA-stilbene to partially or fully Q-extracted chromatophores has no effect on the [2Fe–2S] cluster EPR spectral line shape, resulting in unaltered g_x resonances at 1.783 and 1.765, respectively (data not shown). These observations are of critical importance for interpretation of the original Q-extraction data, since they imply that the origin of the g_x resonance at 1.783 is not due to the inhibitors themselves interacting with the [2Fe–2S] cluster and fortuitously generating the

same EPR spectral line shape as the Q-extracted chromatophores, but rather by specifically displacing ubiquinone from the Q_{OW} domain, resulting in a Q_O site in which only the Q_{OS} domain is occupied.

Extensive kinetic investigations of Q_O site inhibition by DPA imply that it is behaving as a noncompetitive inhibitor of the cyt bc_1 complex function. Similar conclusions have been drawn for MOA-stilbene inhibition of purified bovine mitochondrial cyt bc_1 complex (Brandt *et al.*, 1988, 1991; Brandt and von Jagow, 1991; Brandt and Djafarzadeh-Andabili, 1997). In the latter case, Brandt and co-workers have shown that ubiquinone was still present in the MOA-stilbene-inhibited Q_O site and on this basis proposed that MOA-stilbene disrupted bovine cyt bc_1 complex activity in a noncompetitive manner (Brandt *et al.*, 1988). The EPR and kinetic data we have obtained from *R. capsulatus* chromatophores investigating the nature of MOA-stilbene-mediated Q_O site inhibition completely agrees with this inhibitor exhibiting noncompetitive inhibition (Sharp *et al.*, 1999b). Cocrystals of MOA-stilbene bound in the Q_O site show that it is located toward the cyt b_L heme, but is not involved in any direct interaction, hydrogen bonding, or otherwise, with either of the metal cofactors that flank the Q_O site (Kim *et al.*, 1998). In keeping with this, binding of MOA-stilbene to the Q_O site has very little effect on the thermodynamic properties of the nearby redox cofactors, with a 30 mV lowering in the [2Fe–2S] cluster midpoint potential and no effect on the cyt b_L heme midpoint potential. DPA also has similarly minor effects on the [2Fe–2S] cluster midpoint potential, in this case raising it by 30 mV and no effect on the cyt b_L heme potential (Sharp *et al.*, 1999b).

Correlation between the Biochemical Data and the Cytochrome bc_1 Crystal Structure Data

In the cocrystal of the cyt bc_1 complex and bound MOA-stilbene, the FeS subunit has moved away from the Q_O site, positioning the [2Fe–2S] cluster closer to the cyt c_1 heme (Q_O distal) (Kim *et al.*, 1998). In this structure, the [2F–2S] cluster is appropriately positioned for electron transfer to cyt c_1, but not for accepting electrons from QH_2 in the Q_O site (see later section). When interpreting the structural information in terms of the biochemical experiments with cyt bc_1 complexes in chromatophores, it is important to consider the fact that the structural data was obtained in the absence of any ubiquinone in the Q_O site (Xia *et*

al., 1997; Iwata *et al.*, 1998; Kim *et al.*, 1998; Zhang *et al.*, 1998). A contradiction arises if the crystal structure data is directly compared with the EPR experiments described here, since one would expect the EPR line shape to exhibit a g_x resonance at 1.765 if the FeS position was distal to the Q_O site. In the native complex in the presence of MOA-stilbene (and DPA), the [2Fe–2S] cluster EPR spectral line shape has a g_x resonance at 1.783, implying that the cluster still senses the presence of ubiquinone in the Q_{OS} domain even when ubiquinone in the Q_{OW} domain has been displaced (Fig. 1B). In order for this to occur, the [2Fe–2S] cluster needs to be close to the Q_O site and, as such, we favor a FeS subunit geometry that is proximal to the Q_O site under these conditions. On the basis of this reasoning, we propose that the region of the Q_O site which binds stigmatellin (proximal to the [2Fe–2S] cluster), probably represents the Q_{OS} ubiquinone domain and the region that MOA-stilbene binds to may correlate with the Q_{OW} ubiquinone domain (proximal to cyt b_L).

Noninhibiting Perturbation of Q_O Site Properties

Aside from kinetic measurements, all the above experimental approaches for studying Q_O site function rely on empirical observations concerning the reduced [2Fe–2S] cluster EPR spectral line shape and the sensitivity of this signal to the nature of the Q_O site occupants. We have noted that the [2Fe–2S] cluster EPR spectral signature is also sensitive to the presence of alcohols (Ding *et al.*, 1992; Sharp *et al.*, 1998, 1999c). This is of relevance to the structural data, since glycerol (an alkane triol) is present at 20% v/v in the purification buffers and crystallization media (Xia *et al.*, 1997; Iwata *et al.*, 1998; Kim *et al.*, 1998; Zhang *et al.*, 1998). We have quantitatively examined the effect of ethanol and glycerol in an attempt to rationalize their influence, if any, on Q_O site function (Sharp *et al.*, 1998, 1999c). Figure 4 shows the effect of ethanol and glycerol on the [2Fe–2S] cluster EPR spectral signature in chromatophore membranes containing native amounts of ubiquinone. Addition of ethanol results in broadening of the line shape and an upfield shift of the g_x resonance from 1.800 to 1.773 (Fig. 4). This is not a solvent effect as it reaches saturation around 200 mM ethanol concentration and the binding isotherm is hyperbolic in nature, with 50% saturation being achieved at about 30 mM ethanol (about 5000 times higher than the cyt bc_1 complex concentration,
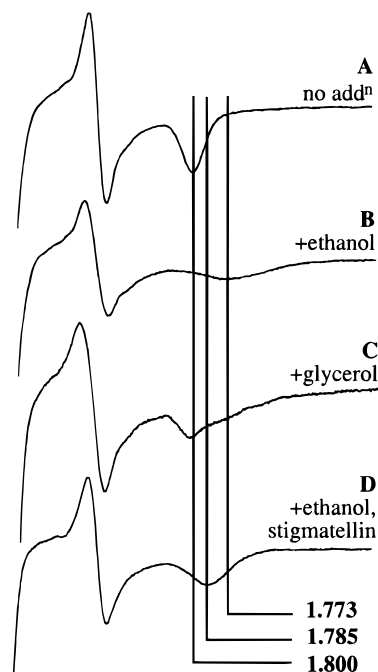

Fig. 4. Effect of alcohols on the EPR spectra of reduced [2Fe–2S] cluster in *R. capsulatus* chromatophores. Experimental details were as for Fig. 3. (A) Native chromatophores suspended in buffer solution; (B) native chromatophores + 170 mM ethanol; (C) chromatophores prepared in buffer solution containing 20% glycerol; (D) + native chromatophores + 20 μM stigmatellin and 170 mM ethanol.

implying that although the interaction is specific, it is rather weak). When partially or fully Q-extracted chromatophore membranes are exposed to ethanol, the same EPR spectral line shape is induced as that for native chromatophores, the g_x resonance shifts from 1.800 to 1.773 (data not shown), implying that ethanol out-competes the interactions of ubiquinone or water with the [2Fe–2S] cluster. Interestingly, in native chromatophore membranes, concentrations of ethanol up to 850 mM have no effect at all upon cyt bc_1 catalysis under a variety of experimental conditions (data not shown). Thus we have termed this effect a *noninhibiting perturbation* of Q_O site function (Sharp *et al.*, 1998). Figure 4 shows the effect on the [2Fe–2S] cluster EPR spectral signature of adding 20% glycerol to native chromatophore membranes. This spectrum is more complicated than that obtained with ethanol and appears to be composed of two components, with g_x resonances at 1.800 and 1.773, and readily interpretable as ethanol and glycerol both having similar effects upon the [2Fe–2S] cluster EPR spectral signature, but to differing extents (Sharp *et al.*, 1999c). The effects

of either alcohol can be completely negated by addition of the tight binding Q_O site inhibitor stigmatellin, which under all conditions induces a characteristic [2Fe–2S] cluster EPR spectral line shape with a g_x resonance at 1.785, essentially by recoupling the [2Fe–2S] cluster to the Q_O site (Fig. 4). The effects of alcohols upon the [2Fe–2S] cluster EPR spectral line shape is interpreted as being due to hydrogen bonding interactions between the $N_\varepsilon H$ atom(s) of the histidine ligands and the alcohol hydroxyl groups. At sufficiently high concentrations, this essentially out-competes the interactions of the [2Fe–2S] cluster histidine ligands with the Q_O site ubiquinones, but interestingly does not hinder cyt bc_1 complex Q_O site function (Sharp *et al.*, 1998). From our experimental data, we suggest that the order of the interaction strengths with the [2Fe–2S] cluster are: stigmatellin $>>$ Q $=$ QH$_2$ $>$ alcohols $>$ water (Sharp *et al.*, 1998).

MODELING ELECTRONS TRANSFER REACTIONS IN THE CYTOCHROME bc_1 COMPLEX: IMPLICATION FOR Q_O SITE CATALYSIS

Now that some structural resolution of the redox centers in the cytochrome bc_1 complex is available, electron tunneling rates between redox centers can be more easily estimated. Tunneling limits electron transfer rates in many intraprotein systems, although the overall rates may be restricted by coupled reactions, such as diffusion. A general empirical expression for the tunneling rate has been derived from extensive manipulation of the multiple reactions of photosynthetic reaction centers (Moser *et al.*, 1992). For an exergonic reaction ($\Delta G < 0$):

$$\log k_{et}^{ex} = 15 - 0.6R - 3.1 (\Delta G^o + \lambda)^2/\lambda$$

where k_{et}^{ex} is the exergonic tunneling rate in s^{-1}; R, the edge-to-edge distance in A; ΔG^o and λ the free energy and reorganization energy of electron transfer in eV. The related endergonic expression reflects a Boltzmann equilibrium penalty:

$$\log k_{et}^{en} = 15 - 0.6R - 3.1 (-\Delta G^o + \lambda)^2/\lambda$$
$$- \Delta G^o/0.06$$

When the structure of the medium between the redox centers is known in detail, it is possible to further refine these calculations to reflect the medium packing density (Page *et al.*, submitted). Redox midpoint poten-

tials of cyt c_1 and the [2Fe–2S] cluster are known, allowing ΔG^o to be directly calculated (Ding *et al.*, 1995; Sharp *et al.*, 1999a). The reorganization energy is less easily defined experimentally, but values between 0.7 and 1 eV typically apply to most reactions inside proteins (Moser and Dutton, 1992). Figure 5 shows the rates of electron tunneling from [2Fe–2S] cluster to cyt c_1 at three edge-to-edge distances found
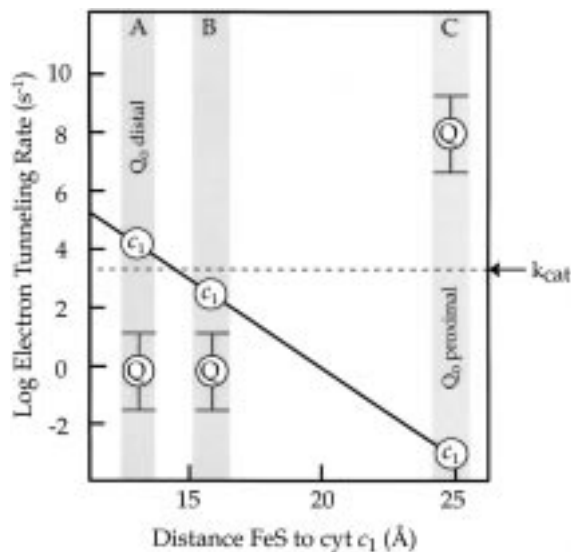

Fig. 5. Correlation of the distance between the [2Fe–2S] cluster and cyt c_1 and the calculated electron-tunneling rates. In position (A), the FeS subunit is distal to the Q_O site and close to cyt c_1, with a 12 A edge-to edge distance between the [2Fe–2S] cluster and the heme macrocycle. This structure is that of bovine cyt bc_1 reported by Zhang *et al* (1998); all other structures used were also reported by Zhang *et al.* (1998). In this position, electron tunneling from the [2Fe–2S] cluster to the cyt c_1 heme is calculated to be 20-fold faster than the turnover number, k_{cat}, which is 1700 s^{-1}. In this structure, electron tunneling from QH$_2$ in the Q_O site to the distal [2Fe–2S] cluster is prohibitively slow. In position (B), the FeS subunit is still distal to the Q_O site but not as close to the cyt c_1 heme as in position (A) (obtained from the structure of the complex isolated from chicken). In position (C), the FeS subunit is proximal to the Q_O site and removed from the cyt c_1 subunit, with a 25 A edge-to edge distance between the [2Fe–2S] cluster and the heme macrocycle (obtained from the chicken structure with bound stigmatellin). In this position, electron tunneling from QH$_2$ in the Q_O site to the [2Fe–2S] cluster is 10^4-fold faster than k_{cat}, but now tunneling from the [2Fe–2S] cluster is prohibitively slow. Key: Q, ubihydroquinone; c_1, cyt c_1; FeS, [2Fe–2S] cluster; k_{cat}, maximum turnover number. All distances measured are the nearest edge-to-edge approaches between the cofactors. The bars on the electron-tunneling rates from QH$_2$ in the Q_O site to the [2Fe–2S] cluster represent the distribution in rates that would be observed for ubiquinones with varying semiquinone stability constants from 10^{-14} to 10^{-20}. The figure is discussed in detail in the text.

in reported crystal structures (Zhang *et al.*, 1998). Only for distances of about 14 A or less (such as that found in the inhibitor-free structure of the complex isolated from bovine heart) can the electron transfer be faster than the observed k_{cat} for QH_2 oxidation and cyt c_1 reduction (Ding *et al.*, 1995). The larger edge-to-edge distances observed in the intermediate FeS position between Q_O site and cyt c_1 (inhibitor-free structure of the complex from chicken) and Q_O site proximal (stigmatellin-containing structures) cannot support rapid enough electron tunneling (Zhang *et al.*, 1998).

Although the average two-electron redox potential of the Q_O ubiquinones are well defined (Ding *et al.*, 1992), the potentials of the individual single-electron couples are dependent on the ubisemiquinone stability constant and are unknown (Ding *et al.*, 1995). However, ubiquinone in the Q_O site appears to be at least as unstable as the Q_{pool} (stability constant has been estimated to be about 10^{-10}), with the actual value for the stability constants likely to be $\leq 10^{-14}$ (Ding *et al.*, 1995). Figure 5 shows the expected electron tunneling rates from QH_2 (near where stigmatellin binds) to the [2Fe–2S] cluster in each of the three structures for a range of stability constant from 10^{-10} to 10^{-18}. Although electron tunneling from the [2Fe–2S] cluster to cyt c_1 is faster than k_{cat} when the FeS subunit position is distal to the Q_O site (Fig. 5), tunneling from QH_2 to the [2Fe–2S] cluster is much slower than k_{cat}. A similarly slow rate is expected in the structure where the FeS subunit position is intermediate between the Q_O site and cyt c_1. Electron tunneling from QH_2 in the Q_O site to the [2Fe–2S] cluster may be as fast as 10^8 sec^{-1} when the FeS subunit is in the Q_O proximal position (stigmatellin geometry), but tunneling from the [2Fe–2S] cluster to cyt c_1 would be likely to take hours. Clearly, the FeS subunit cannot assume a single geometry, which will facilitate rapid electron transfer with both QH_2 in the Q_O site and cyt c_1; the geometry must change on the time scale of k_{cat}, presumably by constrained diffusion of the FeS subunit.

The dimeric nature of the cytochrome bc_1 complex crystal structure places the FeS subunit of one-half of the dimer closer to the cytochromes c_1 and b of the other subunit, indicating interdimer electron transfer at the level of the FeS subunit is possible (Xia *et al.*, 1997; Iwata *et. al.*, 1998; Kim *et al.*, 1998; Zhang *et al.*, 1998). We suggest that interdimer electron transfer can also take place at the level of the b_L hemes, which are separated by an edge-to-edge distance of only 13.3 A. Kinetic simulations using the above equations show that electron tunneling between the b_L

hemes (ΔG^o, 0 eV; λ, 0.7 eV) can occur at a rate of $\sim 7 \times 10^4$ s^{-1}. Thus oxidation of QH_2 at the Q_O site, which initially leads to reduction of b_H in one-half of the dimer, can be followed by an approximately 10 msec equilibration with the cyt b_H on the other half of the dimer by means of electron tunneling between the two cytochromes b_1. This possible intrasubunit equilibration should have experimentally verifiable consequences in partially inhibited systems (Bechmann *et al.*, 1992).

The same tunneling equations can be used to simulate the two sequential electron transfers from QH_2 in the Q_{OS} domain to the oxidized high-(FeS to cyt c_1) and 1ow-potential (cyt b_L to cyt b_H) redox chains, respectively. The overall tunneling rate for the two electron transfers will depend on the instability of the ubisemiquinone states and on the relative amount of time that the FeS subunit spends in the vicinity of Q_{OS} at a distance which is appropriate for rapid electron tunneling. Using distances for nonubiquinone components in crystal structures, and setting the edge-to-edge distance between Q_{OS} and Q_{OW} to about 5 A, tunneling calculations indicate that the stability constant for Q_{OS} can be lower than 10^{-20} and still provide electron transfer rates through Q_{OW} and cyt b_L to cyt b_H faster than the observed k_{cat}, without creating a large transient population of reduced cyt b_L. Indeed, this also provides the conditions which explain that when Q_{OW} is not present (for example, if an inhibitor such as MOA-stilbene replaces Q_{OW}, or the ubiquinone is extracted), electron transfer from Q_{OS} to cyt b_L and on to cyt b_H slows to the seconds time scale, consistent with observed experimental rates (Ding *et al.*, 1995, Sharp *et al.*, 1999b).

CONCLUSIONS AND PERSPECTIVES

From the data summarized in this review, several key features of Q_O site function are revealed:

1. Unless the extensive EPR data we have reviewed can be proved to arise from other sources, then the best model for interpretation of our data is that the Q_O site can accommodate at least two ubiquinone molecules (Ding *et al.*, 1992, 1995; Sharp *et al.*, 1999a, b). The crystal structures of cyt bc_1 complex with stigmatellin and MOA-stilbene bound in the Q_O site are identified as binding these inhibitors proximal to the FeS subunit (stigmatellin) and proximal to cyt b_L (MOA-stilbene), respectively (Kim *et al.*, 1998). On the basis of the data presented here, we propose

that the stigmatellin and MOA-stilbene binding domains may very well correspond to the biochemically observed Q_{OS} and Q_{OW} ubiquinone-binding domains, with the ubiquinone in the Q_{OS} domain behaving as a catalytic cofactor and that in the Q_{OW} domain as a substrate ubiquinone.

2. It is clear that when the [2Fe–2S] cluster is in the reduced state (as in all the EPR experiments), the equilibrium position (K_{eq}) of the FeS subunit is proximal to the Q_O site, as the [2Fe-2S] cluster EPR spectral parameters are highly sensitive to the Q_O site occupants (Robertson *et al.*, 1990; Ding *et al.*, 1992, 1995; Sharp *et al.*, 1998, 1999a, b, c). This seems to be counterintuitive, since during the catalytic cycle of the cyt bc_1 complex before oxidation of QH_2 can be initiated at the Q_O site, the [2Fe–2S] cluster must first be oxidized by cyt c_1. As presented in the last section and from the reported crystals structures, this has to occur by diffusion of the FeS subunit from a Q_O proximal to distal position, because both positions are mutually exclusive in terms of the electron transfer reactions that they support to and from the [2Fe–2S] cluster. However, from modeling the electron tunneling events and with the knowledge that the favored equilibrium position of the reduced [2Fe–2S] cluster is proximal to the Q_O site, we propose that even if movement of the FeS subunit closer to cyt c_1 is energetically unfavored by up to 1.4 Kcal mol^{-1} (where K_{eq} for the proximal position of the FeS subunit is arbitrarily taken to be 10), electron delivery to cyt c_1 can still occur within the time scale of turnover of the cyt bc_1 complex.

3. One question which arises directly from point (2) is whether movement of the FeS subunit is under redox control. EPR spectroscopy is not the best tool to investigate this as only the reduced form of the [2Fe–2S] cluster can be probed; in the future perhaps Fourier-transformed infrared spectroscopy (FTIR) would be a more general tool to complement the EPR analysis. Having stated this, it is evident that the redox midpoint potential of the [2Fe–2S] cluster is independent of the environment of the FeS subunit (except when certain inhibitors are bound in the Q_O site), as the potentials of the isolated FeS subunit and that in the holo enzyme are the same. Furthermore, the redox midpoint potentials of ubiquinone Q_O site occupants are very similar to that of the Q_{pool} (+ 90 mV), indicating that the reduced FeS subunit has equal binding affinity for Q or QH_2 (Ding *et al.*, 1992).

REFERENCES

Bechmann, G., Weiss, H., and Rich, P. R. (1992). *Eur. J. Biochem.* **208**, 315–325.

Brandt, U. (1996a). *FEBS Lett.* **387**, 1–6.

Brandt, U. (1996b). *Biochim. Biophys. Acta* **1275**, 41–46.

Brandt, U. (1998). *Biochim. Biophys. Acta* **1365**, 261–268.

Brandt, U., and Okun, J. G. (1997). *Biochemistry* **36**, 11234–11240.

Brandt, U., and Trumpower, B. (1994). *Crit. Rev. Biochem. Mol. Biol.* **29**, 165–197.

Brandt, U. and von Jagow, G. (1991). *Eur. J. Biochem.* **195**, 163–170.

Brandt, U., and Djafarzadeh-Andabili, R. (1997). *Biochim. Biophys. Acta* **1321**, 238–242.

Brandt, U., Haase, U., Schagger, H., and von Jagow, G. (1991). *J. Biol. Chem.* **266**, 19958–19964.

Brandt, U., Schagger, H., and von Jagow, G. (1988). *Eur. J. Biochem.* **173**, 499–506.

Crofts, A. R., and Berry, E. A. (1998). *Curr. Opin. Struct. Biol.* **8**, 501–509.

Crofts, A. R., and Wang, Z. (1989). *Photosyn. Res.* **22**, 69–87.

Crofts, A. R., and Wraight, C. A. (1983). *Biochim. Biophys. Acta* **726**, 149–185.

Crofts, A. R., Barquera, B., Gennis, R. B., Kuras, R., Guergova-Kuras, M., and Berry, E. A. (1999). In *The Phototrophic Prokaryotes* (Peschek, G. A., Loffelhard, W., and Schmetterer, G., eds.), Plenum, New York, pp. 229–239.

Ding, H., Robertson, D. E., Daldal, F., and Dutton, P. L. (1992). *Biochemistry* **31**, 3144–3158.

Ding, H., Moser, C. C., Robertson, D. E., Tokito, M. K., Daldal, F., and Dutton, P. L. (1995). *Biochemistry* **34**, 15979–15996.

Gray, K. A., and Daldal, F. (1995). In *Anoxygenic Photosynthesis* (Blankenship, R. E., Madigan, M. T., and Bauer, C., eds.), Kluwer Academic Publishers, Dordrecht, The Netherlands, pp. 725–745.

Iwata, S., Lee, J. W., Okada, K., Lee, J. K., Iwata, M., Rasmussen, B., Link, T. A., Ramaswamy, S., and Jap, B. K. (1998). *Science* **281**, 64–71.

Junemann, S., Heathcote, P., and Rich, P. R. (1998). *J. Biol. Chem.* **273**, 21603–21607.

Kim, H., Xia, D., Yu, C.-A., Xia, J.-Z., Kachurin, A. M., Zhang, L., Yu, L., and Deisenhofer, J. (1998). *Proc. Natl. Acad. Sci. U.S.* **95**, 8026–8033.

Lawford, H. G., and Garland, P. B. (1983). *Biochem. J.* **130**, 1029–1044.

Mitchell, P. (1975). *FEBS Lett.* **59**, 137–139.

Moser, C. C. and Dutton, P. L. (1992). *Biochim. Biophys. Acta* **1101**, 171–176.

Moser, C. C., Keske, J. M., Warncke, K., Farid, R. S., and Dutton, P. L. (1992). *Nature* **355**, 796–802.

Page, C C., Moser, C. C., Chen, X., and Dutton, P. L., submitted to *Nature*.

Robertson, D. E., Daldal, F., and Dutton, P. L. (1990). *Biochemistry* **29**, 11249–11260.

Sharp, R. E., Palmitessa, A., Gibney, B. R., Moser, C. C., Daldal, F., and Dutton, P. L. (1998). *FEBS Lett.* **431**, 423–426.

Sharp, R. E., Palmitessa, A., Gibney, B. R., White, J. L., Moser, C. C., Daldal, F., and Dutton, P. L. (1999a). *Biochemistry* **38**, 3440–3446.

Sharp, R. E., Palmitessa, A., Gibney, B. R., Moser, C. C., Daldal, F., and Dutton, P. L. (1999b). *Biochem. Soc. Trans.*, in press.

Sharp, R. E., Palmitessa, A., Gibney, B. R., Moser, C. C., Daldal, F., and Dutton, P. L. (1999c). In *The Phototrophic Prokaryotes* (Peschek, G. A., Loffelhard, W., and Schmetterer, G., eds.), Plenum, New York, pp. 241–250.

Xia, D., Yu, C. A., Kim, H., Xia, J. Z., Kachurin, A. M., Zhang, L., Yu, L., and Deisenhofer, J. (1997). *Science* **277**, 60–66.

Zhang, Z., Huang, L., Shulmeister, V. M., Chi, Y. I., Kim, K. K., Hung, L. W., Crofts, A. R., Berry, E. A., and Kim, S. H. (1998). *Nature* **392**, 677–684.